

Large Scale Fluctuations in the X-Ray Background

Marie Treyer¹, Caleb Scharf², Ofer Lahav³, Keith Jahoda⁴, Elihu Boldt⁴, Tsvi Piran⁵

¹ Astrophysikalisches Institut Potsdam, An der Sternwarte 16, 14842 Potsdam, Germany,
 mtreyer@aip.de

² Space Telescope Science Institute, 3700 San Martin Drive, Baltimore, MD 21218,
 scharf@stsci.edu

³ Institute of Astronomy, Madingley Road, Cambridge CB3 OHA, U.K.;
 lahav@ast.cam.ac.uk

⁴ Laboratory of Hight Energy Astrophysics, NASA/GSFC, Greenbelt, MD 20771,
 keith@pcasrv2.gsfc.nasa.gov, boldt@lheavx.gsfc.nasa.gov

⁵ Racah Institute of Physics, The Hebrew University, Jerusalem 91904, Israel,
 tsvi@shemesh.fiz.huji.ac.il

ABSTRACT

We present an attempt to measure the large angular scale fluctuations in the X-Ray Background (XRB) from the HEAO1 A2 data, expressed in terms of spherical harmonics. We model the harmonic coefficients assuming a power spectrum and an epoch-dependent bias parameter, and using a phenomenological scenario describing the evolution of the X-ray sources. From the few low-order multipoles detected ($l < 10$), we estimate the power-spectrum normalisation on scales intermediate between those explored by local galaxy redshift surveys ($\sim 100h^{-1}$ Mpc) and by the COBE Microwave Background measurements ($\sim 1000h^{-1}$ Mpc). We find that the HEAO1 harmonics are consistent with present epoch rms fluctuations of the X-ray sources $b_x(0)\sigma_8 \sim 1 - 2$ in $8 h^{-1}$ Mpc spheres. Therefore the observed fluctuations in the XRB are roughly as expected from just interpolating between the fluctuations in local galaxy surveys and the COBE CMB. We predict that an X-ray whole sky surface brightness survey which resolves sources a factor of 10 fainter than HEAO1, would allow us to measure the large scale fluctuations of the XRB to order $l \sim 20$ (on angular scale $\theta \sim \pi/20$), and therefore more strongly constrain the large scale structure of the Universe on scales of hundreds of Mpc.

Subject headings: X-rays: diffuse radiation — cosmology: observations, large-scale structure of universe

1. Introduction

Although discovered before the Cosmic Microwave Background (CMB), the origin of the hard X-Ray Background (XRB) is still not fully understood. At energies below 2 keV, the XRB has now been almost entirely resolved into discrete sources, essentially AGN's, although other types of sources (e.g. clusters, narrow emission line galaxies) are also thought to contribute a significant fraction of the total flux (Hasinger et al 1998, McHardy et al. 1998). But the X-ray spectra of these sources are, for the most part, too soft to account for the shape and total intensity of the XRB above 2 keV. Absorption, however, can remedy this problem and allow the full energy range of the XRB to be nicely fitted by the right mixture of absorbed and unabsorbed AGN's (Comastri et al. 1995).

Even if the detailed nature of the hard X-ray sources, and their relation to the soft ones, are not yet fully understood, it is nevertheless believed that the XRB at high energies does arise from the integrated emission of discrete sources, as the alternative hypothesis of a cosmic hot gas origin was ruled out by the observation of the undistorted CMB spectrum (see Fabian & Barcons 1992 for review).

X-ray sources must be found throughout a large volume of the universe in order to account for the observed integrated flux (local X-ray sources only produce a very small fraction of the total flux), making them convenient tracers of the mass distribution on scales intermediate between those in the CMB as probed by COBE (~ 1000 Mpc), and those probed by optical and IRAS redshift surveys (~ 100 Mpc). In terms of the level of anisotropy, the XRB is also intermediate between CMB fluctuations ($\sim 10^{-5}$ on angular scales of degrees) and galaxy density fluctuations (of the order of unity on scale of $8 h^{-1}$ Mpc). The CMB fluctuations originate from redshift $z \sim 1000$. They are due to the Sachs-Wolf effect on scales larger than a few degrees. On the other hand, the fluctuations in the XRB are due to fluctuations in the space density of X-ray sources, which are probably distributed at $z \sim 1 - 5$.

Here we attempt a comparison of the hard band (2-10 keV) XRB fluctuations seen in the HEAO1 A2 data with a range of models. We measure the fluctuations in terms of spherical harmonics coefficients, and make predictions for the ensemble average of these coefficients using a formalism presented by Lahav, Piran & Treyer (1997) (hereafter LPT97). For related approaches see Boughn, Crittenden & Turok (1997) and Barcons, Fabian and Carrera (1997). The data analysis and the theoretical formalism are described in Sections 2 and 3 respectively. Measurements and models are compared in Section 4. We present our conclusions in Section 5. For simplicity, we shall assume an Einstein-de Sitter world geometry, i.e. $\Omega = 1$, and cosmological constant $\Lambda = 0$. We write the Hubble constant as $H_0 = 100 h$ km/s/Mpc.

2. The HEAO1-A2 Data Analysis

Details of the HEAO1-A2 data analysis are described in a complementary paper (Scharf et al., in preparation). This section summarizes the procedure.

We use the A2 counts from the 6 months following day 322 of 1977 in the all-sky survey (c.f. Jahoda 1993). The data was provided in rectangular ecliptic coordinates in approximately 0.5×0.25 degree pixels (at ecliptic equator). This data is then corrected for a small systematic instrumental change from day ~ 430 onwards. In this work we further bin the data into groups of 12 by 12 pixels (smaller resolution pixels are strongly correlated due to the instrument beam) for all analyses. At the ecliptic equator the pixel groups are therefore $6^\circ \times 3^\circ$. Masking (see below) is however performed initially on the higher resolution data and the final pixel groups contain the *mean* count rate of all non-zero ‘sub-pixels’ and are weighted according to their area.

It is difficult to unambiguously separate foreground (Galactic) from background (extragalactic) information in the HEAO1 X-ray data. The total number of resolved foreground and background sources ($|b| > 20^\circ$) is small ($\sim 0.01\text{deg}^{-2}$) and a detailed model of possible large scale Galactic emission is hard to determine. The Galactic 2-10 keV emission model of Iwan et al (1982) predicts variations of no more than 3% of the total flux due to smoothly distributed emission of Galactic origin at the latitudes $|b| > 20^\circ$ considered at the our study.

Studies in the soft bands (< 0.75 keV) by ROSAT (Snowden 1996) indicate that, at these lower energies, the picture is more complicated, with Galactic emission at all scales. In this present work, as a first step towards removing the foreground we construct a ‘mask’ using a list of resolved and identified (Piccinotti et al. 1982) Galactic X-ray sources and a $|b| < 20^\circ$ Galactic Plane mask. Regions of sizes varying from $\sim 8^\circ$ diameter to 12° diameter are excised around resolved sources, larger regions are removed around the Large and Small Magellanic Clouds (LMC, SMC). A total of $\sim 23\%$ of the raw all-sky flux is removed by this ‘Galactic’ mask.

The removal of bright extragalactic sources is important in order to control shot-noise in the angular power estimates (LPT97). We attempt to do this by further masking out all 61 extragalactic (AGN and cluster) sources in the catalogue of Piccinotti et al (1982), to a flux limit of $S_{cut} = 3 \times 10^{-11} \text{ erg s}^{-1} \text{ cm}^{-2}$ (2-10 keV). The final unmasked area is then $\sim 55\%$ of the sky with an effective $z_{min} \sim 0.02$ (approximately the median redshift of the Piccinotti sources).

Finally, the dipolar contribution to the anisotropy due to the motion of the observer with respect to the XRB, the Compton-Getting (CG) effect, is subtracted from the flux

(Boldt 1987, Jahoda 1993, LPT97). The amplitude of this dipole is estimated from the observed motion with respect to the CMB and the observed hard XRB spectral power index ($\alpha = 0.4$). We note that the raw HEAO1 dipole (Galactic sources and plane removed), due to both the CG effect and large scale structure (see LPT97), points in the direction $l \approx 330^\circ; b \approx 33^\circ$. This can be compared with the CMB dipole (in the Local Group frame) which points towards $l \approx 268^\circ; b \approx 27^\circ$ (based on COBE, Lineweaver et al. 1996). We shall further discuss the HEAO1 dipole elsewhere (Scharf et al., in preparation). The HEAO1 data are then expanded in spherical harmonics and the harmonic coefficients determined (Scharf et al. 1992, LPT97).

3. Modeling

To model the large angular scale fluctuations in the XRB, we follow the formalism proposed by LPT97 using the following new set of assumptions:

(i) X-ray light traces mass, and we assume linear, epoch-*dependent* biasing between the spatial fluctuations in the X-ray source distribution, δ_x , and those of in the underlying mass distribution, δ_M : $\delta_x(z) = b_x(z)\delta_M(z)$. We adopt the following prescription (Fry 1996) for the time-dependence of the biasing parameter, which we parametrize in terms of the present-epoch parameter $b_x(0)$:

$$b_x(z) = b_x(0) + z[b_x(0) - 1] \quad (1)$$

This assumption is somewhat more realistic than the time-independent bias parameter used by LPT97. In Fry's model the galaxies were formed at an early epoch z_* in a biased way, and then clustered with time under the influence of gravity. Note that if $b_x(z_*) = 1$ then $b_x(0) = 1$. However, if $b_x(z_*) > 1$, biasing decreases with cosmic epoch (see also Bagla 1997).

(ii) Although we assume an Einstein-de Sitter cosmology ($\Omega = 1, \Lambda = 0$), we use a phenomenological low-density CDM model (with a shape parameter $\Gamma = 0.2$) to represent the present-day power-spectrum $P(k) \equiv \sigma_8^2 \bar{P}(k)$, where σ_8 is the present-epoch normalization of the mass fluctuations in $8h^{-1}$ Mpc spheres. In this case the mass power-spectrum evolves according to linear theory as $P(k, z) \propto (1+z)^{-2}$. For the X-ray light fluctuations, $\delta_x(\mathbf{k}, z)$, these assumptions translate into:

$$\langle \delta_x(\mathbf{k}) \delta_x^*(\mathbf{k}') \rangle(z) = (2\pi)^3 \sigma_8^2 b_x^2(z) \bar{P}(k) (1+z)^{-2} \delta^{(3)}(\mathbf{k} - \mathbf{k}'), \quad (2)$$

where $\delta^{(3)}$ is the three-dimensional delta-function.

(iii) The X-ray intensity observed in the 2-10 keV energy band originates from the integrated emission of discrete X-ray sources out to some high redshift z_{max} . We describe this population by its local luminosity function $\phi_x(L)$ and spectral index α , and assume simple power-law evolution both in luminosity: $L(z) \propto (1+z)^e$, and in number density: $\phi(L, z) \propto (1+z)^d$. The local X-ray light density is:

$$\rho_0 = \int_0^\infty L \phi_x(L) dL, \quad (3)$$

and the X-ray light density at redshift z observed in the 2-10 keV energy range is:

$$\rho_x(z) = \rho_0 (1+z)^q \quad (4)$$

where $q = d + e - \alpha + 1$.

With these assumptions, we predict the ensemble average of the spherical harmonics coefficients of the XRB. The total predicted signal result in a large scale structure component, reflecting the underlying mass distribution, and a shot noise component due to the discreteness of the sources (as opposed to the continuous mass distribution):

$$\langle |a_l^m|^2 \rangle_{model} = \langle |a_l^m|^2 \rangle_{LSS} + \langle |a_l^m|^2 \rangle_{sn} \quad (5)$$

The shot noise term is:

$$\langle |a_l^m|^2 \rangle_{sn} = \frac{1}{4\pi} \sum_{sources} S_i^2 = \int_0^{S_{cut}} S^2 N(S) dS \quad (6)$$

where $N(S)$ is the differential number-flux relation of the X-ray sources. Bright sources (brighter than a suitable flux cutoff S_{cut}) must be removed to reduce the shot noise. However, removing sources also reduces the large scale structure signal.

The large scale structure component can be written as an integral over the power spectrum (LPT97):

$$\langle |a_l^m|^2 \rangle_{LSS} = \frac{(r_H \rho_0)^2}{(2\pi)^3} \int k^2 \bar{P}(k) |\Psi_l(k)|^2 dk \quad (7)$$

where $r_H = c/H_0$ is the Hubble radius and the window function Ψ_l contains the model parameters:

$$\Psi_l(k) = \int_0^{z_{max}} \sigma_8 b_x(z) (1+z)^{q-9/2} j_l(kr_c) W_{cut}(z) dz. \quad (8)$$

The function $W_{cut}(z)$ accounts for the removal of sources brighter than S_{cut} :

$$W_{cut}(z) = \frac{1}{\rho_0} \int_0^{L_{cut}(z)} L \phi_x(L) dL \quad (9)$$

where:

$$L_{cut}(z) = 4\pi r_c^2(z) S_{cut}(1+z)^{\alpha+1-e}. \quad (10)$$

$r_c(z)$ is the comoving radial distance. For the monopole ($l = 0$), we recover the ‘Olbers integral’: $A_0 = \langle |a_0^0|^2 \rangle_{LLS}^{1/2} = \bar{I} \sqrt{4\pi}$, where \bar{I} is the mean total intensity of the XRB. In a flat universe and for $q \neq 2.5$, Eq. 4 implies:

$$\bar{I} = \frac{\rho_0 r_H}{4\pi} \times \frac{(1+z_{max})^{q-2.5} - 1}{q - 2.5}. \quad (11)$$

The higher order multipoles characterize the spatial fluctuations of the XRB on angular scales $\sim \pi/l$.

In order to compare model expectations with HEAO1 observations, we further convolve our predictions with the foreground masks described above:

$$\langle |c_l^m|^2 \rangle = \sum_{l'm'} |W_{ll'}^{mm'}|^2 \langle |a_{l'm'}|^2 \rangle, \quad (12)$$

where the $W_{ll'}^{mm'}$ tensor models the mask (Peebles 1980, Scharf et al. 1992, Baleisis et al. 1997). Finally, the predicted masked harmonics and shot noise are normalized over the monopole. We use the following notation:

$$C_{sn} = \frac{\langle |c_l^m|^2 \rangle_{sn}^{1/2}}{A_0} \quad (13)$$

for the shot noise, and for the full signal:

$$C_l = \frac{(\langle |c_l^m|^2 \rangle_{LSS} + \langle |c_l^m|^2 \rangle_{sn})^{1/2}}{A_0}. \quad (14)$$

4. Observational Constraints

The local luminosity function in the 2 – 10 keV energy band can be fit by a double power-law function between $L_{min} \approx 10^{42}$ and $L_{max} \approx 10^{48} h^{-2}$ ergs s $^{-1}$ (Grossan 1997, Boyle et al. 1997). The integrated emission of local sources (with $L_{min} < L < L_{max}$) is: $\rho_0 \approx 10^{39} h$ ergs s $^{-1}$ Mpc 3 . The total intensity of the 2 – 10 keV XRB is $\bar{I} = 5.2 \times 10^{-8}$ ergs s $^{-1}$ cm 2 sr $^{-1}$, and the spectral index of the spectrum in this energy band is $\alpha = 0.4$ (Boldt 1987).

Boyle et al. (1997) find evidence for strong cosmological evolution matching a pure luminosity evolution model $L_x \propto (1+z)^e$ with $e \approx 2$ out to a redshift of 2, followed by a declining phase. This scenario however, doesn’t account for the total background intensity,

and thus requires other processes or populations whose X-ray emission would add to that currently observed. In the absence of better evidence, we shall make the *ad hoc* assumption that luminosity evolution, as described above, is sustained to a redshift high enough to make up the whole XRB intensity, i.e. $z_{max} \approx 6.4$ (Eq. 11). On the other hand, Hasinger (1997) argues that strong *number* density evolution: $\phi_* \propto (1+z)^d$, provides a better fit to the ROSAT deep sky survey data, with $d \approx 4$, implying that the whole XRB will be accounted for at $z_{max} \approx 1.3$. We shall assume that realistic models range between these two evolution scenarios.

We compute the differential number counts relation for both models. Both are in good agreement with the Euclidean curve, $N(S) \propto S^{-2.5}$, derived from ASCA deep sky observations to $S \sim 5 \times 10^{-14}$ ergs $s^{-1}cm^{-2}$ (e.g. Georgantopoulos et al. 1997). At fainter fluxes the predicted log- N -log- S curves slightly bend down to $S \sim 5 \times 10^{-16}$ ergs $s^{-1}cm^{-2}$, at which flux the total intensity of the XRB is accounted for. From these number counts, we derive the shot noise level as a function of flux cutoff (Eq. 6).

5. Results

Figure 1 shows the normalised XRB harmonics measured through the ‘Galactic’ mask (upper panel) and through the full, foreground removed mask (lower panel) respectively. The lower shot noise from bright source removal is immediately apparent as a lowering in the overall harmonic amplitude. We have assumed a low density CDM model with a shape parameter $\Gamma = 0.2$ and normalization $\sigma_8 = 1.0$ and left the present-epoch biasing parameter $b_x(0)$ (Eq. 1) as a free parameter. We then derived the optimal $b_x(0)$ by Maximum Likelihood (neglecting the mask, cf. Scharf et al. 1992) over the harmonics $1 \leq l \leq 10$. Both evolution scenarios yield the same estimate: $b_x(0) = 1.6$ for the Galactic mask, and $b_x(0) = 1.0$ for the full mask. To bracket the range of estimates, predictions are plotted for these 2 values on both panels (Galactic mask and full mask): the dotted lines represent the density evolution scenario ($q = 4.5$) and the long-dashed lines show the luminosity evolution scenario ($q = 2.5$). Upper lines on both panels are for $b_x(0) = 1.6$ and lower lines for $b_x(0) = 1.0$. Assuming a standard CDM power spectrum yield $b_x(0) = 1.8$ and 1.2 for Galactic and full masks, respectively. This is not surprising, as low density CDM has more power on large scales than standard CDM. For most of the models considered above, the reduced χ^2 is near unity, suggesting acceptable fits.

In the above models, the shot noise levels (masked and normalised) were calculated a priori. Both evolution scenarios yield similar values within 5%. Masking induces the constant shot noise to decrease slightly (by less than 10%) towards the high l ’s. As the

difference between the evolution scenarios and the gradient due to masking are practically undistinguishable, we plot the mean shot noise value as one horizontal line on both panels in Fig. 1: for $S_{cut} = 3 \times 10^{-10} \text{ ergs s}^{-1} \text{ cm}^{-2}$ (i.e no extragalactic sources removed), $C_{sn} \approx 1.1 \times 10^{-3}$; for $S_{cut} = 3 \times 10^{-11} \text{ ergs s}^{-1} \text{ cm}^{-2}$ (i.e. the flux limit of the Piccinotti et al. 1982 catalog), $C_{sn} \approx 5.2 \times 10^{-4}$. These predictions are in very good agreement with the flattening of the measured signal in both cases. We verified it by Maximum Likelihood analysis over harmonics $10 \leq l \leq 20$, by ignoring the clustering term and leaving the shot-noise level as a free parameter. We find that the derived shot-noise for both masks fit to within 10 % of the one predicted from the counts.

However, the measured multipoles do show more curvature as a function of l than our models predict. This may be explained by a number of reasons: the low order multipoles measured in the XRB may result from local (Galactic?) structures unaccounted for by the masks; source clustering evolution may be significantly stronger than the linear theory assumption we have made; or else, the evolution parameters we have used for the X-ray source population are overestimated, at least on part of the redshift range. We note that epoch-dependent biasing improves the fit to the data (see the top panel in Figure 1). We attempted a Maximum Likelihood over the range $1 \leq l \leq 20$ with 2 parameters: $b_x(0)$ and the shot noise level C_{sn} . The 2 parameters are strongly coupled (if $b_x(0)$ is higher, then C_{sn} is lower, and vice versa). Assuming for instance a low density CDM model and $q = 2.5$ for the evolution parameter, and in the case of the Galactic mask, freezing $b_x(0)$ to its best fit value 1.6 (derived above assuming the predicted shot-noise level) would require the normalized shot noise C_{sn} to be 20% smaller than that predicted from the source counts. On the other hand, $b_x(0) = 1.0$ would require C_{sn} to be 10% larger than predicted. The deviations are larger for the full mask, e.g. freezing $b_x(0)$ to its best fit value 1.0 would require C_{sn} to be 30% smaller than that predicted. The trend reflects the strong curvature at low l 's, as discussed above.

Figure 2 shows the corresponding signal to noise as a function of l , assuming $b_x(0) = 1$ and $\sigma_8 = 1$ for the purpose of illustration. In order to compare the above models with predictions at fainter flux limits, we do not use the existing masks. In the lower two panels, we show the signal to noise expected if sources brighter than $S_{cut} = 3 \times 10^{-12}$ and $3 \times 10^{-13} \text{ ergs s}^{-1} \text{ cm}^{-2}$ respectively (i.e. 1 and 2 magnitudes lower than the present data) could be removed from the X-ray whole sky survey. We predict the signal to noise to increase as S_{cut} decreases. The multipoles are also expected to be detectable above shot noise for an increasing range of l . As the present results suggest $b_x(0) \geq 1$, the signal to noise plotted here may be taken as lower limits. Luminosity evolution and density evolution become increasingly distinct as we remove fainter and fainter sources. If sources evolve in luminosity, a given flux cutoff will span a larger redshift range than if they don't or if

they only evolve in number, and therefore a larger volume of space will be excluded from the analysis. Hence a weaker signal to noise in the case of luminosity evolution than in the case of density evolution. We conclude that an X-ray whole sky survey in the hard band (to minimize Galactic contamination) resolving sources only one magnitude fainter than HEAO1, would allow us to measure the large scale fluctuations of the background to significantly higher order l , and therefore to more strongly constrain the large scale structures of the Universe on scales of hundreds of Mpc.

6. Discussion

We report on the possible detection of low-order spherical harmonic modes in the HEAO1 XRB map. Although one must be cautious about the interpretation of the signal as being purely extragalactic, it is encouraging that the measurements are in accord with *a priori* predictions. On the whole, our conclusion is that the XRB fluctuations on scales of few hundreds of Mpc are consistent with what is expected by interpolating between fluctuations from local galaxy surveys and the COBE CMB measurements.

The present analysis allows for epoch-dependent biasing, which seems to give a more reasonable fit than a time-independent biasing scheme. We tested two extreme models for the evolution of the X-ray sources. For both models, the window functions $\Psi_l(k)$ (Eq. 8), for $l \leq 10$, peak in the range of comoving scales $k = 0.001 - 0.01 h \text{ Mpc}^{-1}$ (see e.g. Fig. 1 in LPT97 for the quadrupole window function).

Various models for fluctuations and evolution yield present-epoch biasing factor of typically $b_x(0) \sim 1 - 2$. Regarding models of density fluctuations, as expected the low density CDM model requires lower $b_x(0)$ than standard CDM, which has less power on large scales. We note that our values for the local bias factor $b_x(0)$ are smaller than those derived from the dipole anisotropy of the local AGN distribution (Miyaji 1994) and from HEAO1 assuming epoch-independent biasing (Boughn et al. 1997). Our estimates of $b_x(0)$ from HEAO1 are used elsewhere (Wu, Lahav & Rees, in preparation) to show that the fractal dimension of the universe is very close to 3 on the very large scales.

We predict that an X-ray whole sky survey resolving sources a factor of 10 fainter than HEAO1, would allow us to measure the large scale fluctuations of the XRB to order $l \sim 20$ ($\theta \sim \pi/20$). The present data cannot be used with lower flux thresholds as our method of eliminating sources also reduces sky coverage. The smallest beams on the A2 experiment had $6^\circ \times 3^\circ$ and $6^\circ \times 6^\circ$ fields of view (FWZI) (Boldt 1987); our algorithm for masking out sources removed a patch of sky somewhat larger than the entire field of view. There are

two experimental approaches which can allow a similar analysis to be done while employing a lower flux threshold, thus reducing the shot noise, and allowing a significant measurement of large scale structure over a larger range of l values.

Barcons et al. (1997) propose an experimental concept that maps the X-ray sky with a collimated proportional counter, substantially similar to the A2 experiment, but with a smaller field of view. Such an experiment can mask individual sources with a smaller penalty in terms of sky coverage (and signal) and can therefore mask a larger number, reaching a fainter limiting flux. Such an experiment cannot identify sources an order of magnitude fainter than our flux threshold by itself, and therefore would rely on an externally produced catalog such as that produced by the ABRIXAS survey (Trümper 1998). The advantages of this approach are the relatively small size and simplicity of the experiment.

Jahoda (1998) proposes an array of imaging telescopes, capable of identifying sources nearly two orders of magnitude fainter than the flux limit in the current study, while collecting enough diffuse flux to measure the surface brightness to 1% per square degree, comparable to the Barcons et al. experiment. Imaging allows sources to be removed without affecting sky coverage. This approach requires a substantially larger collecting area than the Barcons et al. approach as critical angle effects make it difficult to build an X-ray mirror that reflects X-rays above 2 keV over its entire geometrical collecting area (Serlemitsos & Soong 1996). The advantages of this approach are the ability to identify and remove sources from this data set directly (eliminating questions about source variability), and the simultaneous production of the deepest all sky, hard X-ray selected catalog ever produced ($> 150,000$ sources selected above 2 keV).

The authors thank B. Boyle, M. Rees and K. Wu for helpful discussions.

REFERENCES

Bagla, J. 1997, preprint, astro-ph/9711081.
Baleisis, A., Lahav, O., Loan, A. & Wall, J.V. 1998, MNRAS, submitted, astro-ph/9709205.
Barcons, X., Fabian, A.C., Carrera, F. 1997, MNRAS 285, 820.
Boldt, E. A. 1987, Phys. Reports, 146, 215.
Boughn, S., Crittenden, R. & Turok, N. 1997, astro-ph/9704043.
Boyle B.J., Georgantopoulos, I., Blair, A.J., Stewart, G.C., Griffiths, R.E., Shanks, T., Gunn, K.F., Almaini, O. 1997, preprint, astro-ph/9710002.

Comastri, A., Setti, G., Zamorani, G., Hasinger, G. 1995, A&A 296, 1.

Fabian, A. C., Barcons, X. 1992, ARA&A, 30, 429.

Fry, J. 1996, ApJ, 461, L65.

Georgantopoulos, I., Stewart, G., Blair, A., Shanks, T., Griffiths, R.E., Boyle, B., Almaini, O., Roche, N. 1997, MNRAS 291, 203.

Grossan, B.A. 1992, Ph.D. thesis, MIT.

Hasinger, G. 1998, Astron. Nachr 319, 37.

Hasinger, G., Burg, R., Giacconi, R., Schmidt, M., Trümper, J., Zamorani, G. 1998, A&A, 329, 482.

Iwan, D., Shafer, R.A., Marshall, F.E., Boldt, E.A., Mushotzky, R.F., Stottlemeyer, A. 1982, ApJ, 260, 111.

Jahoda, K. 1993, Adv. Space Res., 13, (12) 231.

Jahoda, K. 1998, in X-ray Surveys, Potsdam meeting, in press.

Lahav, O., Piran, T., Treyer, M. A. 1997, MNRAS, 284, 499 (LPT97).

Lineweaver, C., Tenorio, L., Smoot, G., Keegstra, P., Banday, A., Lubin, P. 1996, ApJ, 470, 38.

McHardy, I. et al. 1998, Astron. Nachrichten, 319, 51.

Miyaji, T. 1994. PhD thesis, University of Maryland.

Peebles, P.J.E. 1980, Large Scale Structure of the Universe (Princeton University Press).

Piccinotti, G., Mushotzky, R. F., Boldt, E. A., Holt, S. S., Marshall, F. E., Serlemitsos, P. J., Shafer, R. A. 1982, ApJ, 253, 485.

Scharf, C. A., Hoffman, Y., Lahav, O., Lynden-Bell, D. 1992, MNRAS, 256, 229.

Serlemitsos, P.J., & Soong, Y. 1996, Astrophysics and Space Science, 239, 177.

Snowden, S. L. 1996, in Røntgenstrahlung from the Universe, eds. Zimmermann, H.U., Trümper, J., and Yorke, H., MPE Report 263, 299.

Trümper, J. 1998, in X-ray Surveys, Potsdam meeting, in press.

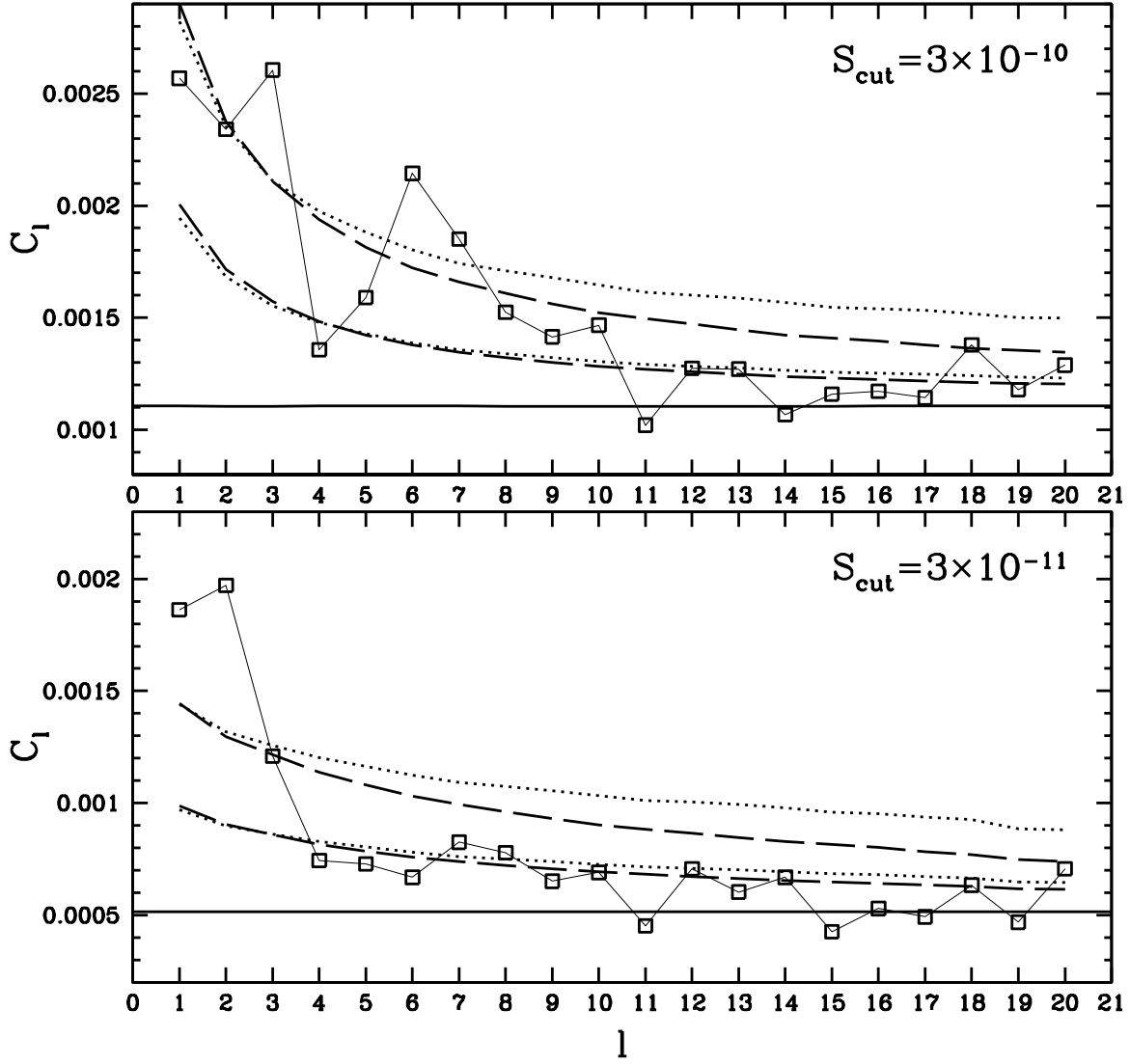


Fig. 1.— The normalised spherical harmonics spectrum of the HEAO1 XRB (squares). In the upper panel, only the Galactic component was removed from the data. In the lower panel, extragalactic X-ray sources from the Piccinotti et al. 1982 catalogue were also removed. The corresponding flux cutoffs S_{cut} in $\text{ergs s}^{-1}\text{cm}^{-2}$ and predicted levels of shot noise (horizontal lines) are indicated in both cases. The dotted lines are the predictions (Eq. 5) of a pure density evolution model ($q = 4.5$), and the long-dashed lines are the predictions of a pure luminosity evolution model ($q = 2.5$). A low density CDM power-spectrum with normalization $\sigma_8 = 1$ for the mass fluctuations was assumed. Upper lines on both panels are for present-epoch biasing parameter $b_x(0) = 1.6$ and lower lines for $b_x(0) = 1.0$.

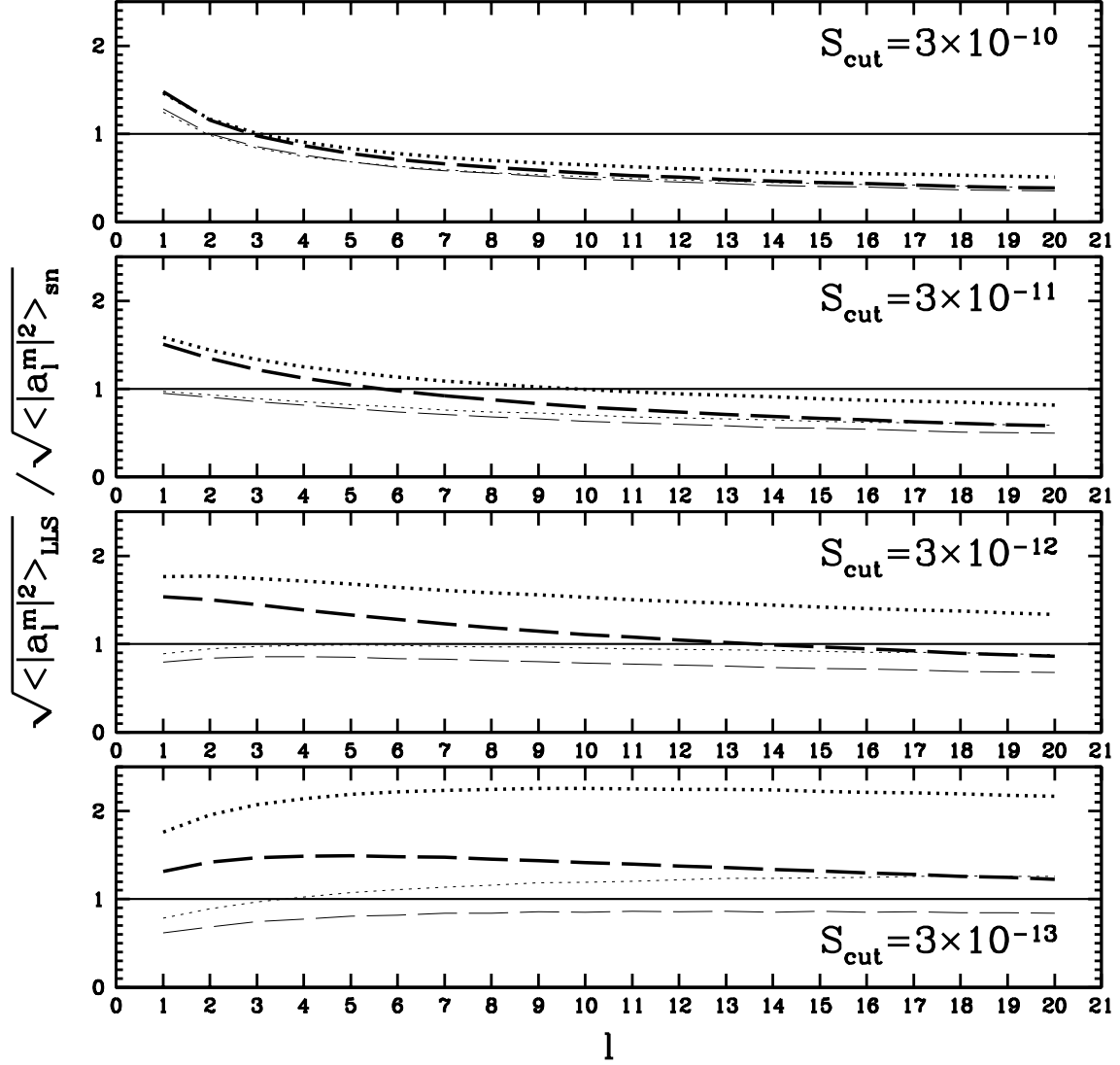


Fig. 2.— Predicted signal to noise as a function of l for decreasing flux cutoffs S_{cut} (as indicated on each panel in $\text{ergs s}^{-1}\text{cm}^{-2}$). We assumed $b_x(0) = 1$ and $\sigma_8=1$. The dotted lines are the predictions of a pure density evolution model ($q = 4.5$), and the long-dashed lines are the predictions of a pure luminosity evolution model ($q = 2.5$). The thick lines assume a low density CDM power spectrum as described in the text. The thinner lines correspond to a standard CDM power-spectrum, for comparison. The horizontal line (signal/noise = 1) marks the shot-noise level.